As originally published in the SMTA Proceedings.

Comparative study of Lead-Free Solder Materials for Power Module Packaging Assembly

Tyler Richmond, Hongwen Zhang, Francis Mutuku,
Jie Geng, Huaguang Wang, Kyle Aserian
Indium Corporation
NY, USA
trichmond@indium.com; hzhang@indium.com

ABSTRACT
The usage of high power devices in electrical vehicles or high temperature electronics requires the interconnection of components to maintain long-term joint integrity under junction temperatures up to 175 °C. Ag- or Cu-sintering materials exhibit excellent thermal and electrical performance, and improved efficiency compared to solder materials. Due to their favorable properties and high melting temperatures, they have been used for die-attach in power inverters/converters. However, the high material and processing costs limit their general usage in the power industry. Alternatively, traditional lead-free solder materials may present challenges for these high power or high temperature devices although they are widely used in electronics interconnections. The high junction temperature and/or service temperature (175 °C or above) in the device leads to homologous temperatures of as high as 0.91. This close to the critical melting point, atomic diffusion is exacerbated and creep resistance is significantly weakened. This has adverse effects on joint reliability as the thermal migration under elevated temperatures promotes grain coarsening, excessive intermetallic compound (IMC) growth, and phase segregation. Electro-migration can also occur if an electrical current is involved. This current study focused on the thermal fatigue performance and the microstructural evolution of five lead-free solders: Sn3.5Ag, Sn5Sb, SnAgCu5.5Sb, SnSbCuAg, and BiAgX® under harsh service conditions. The solder joints were subjected to Temperature Cycling Tests (TCT) of -40 to 175 °C for up to 2000 cycles and 210 °C aging up to 240 hours. 5x5mm^2 Si die (Ti/Ni/Ag metallization) on direct-bonded-Cu (DBC) packages were used for TCT. Aging tests were performed with a Cu die on a ceramic substrate. The ceramic substrate had two different metallization types: (1) electrolytic Ni-plated Cu and (2) electroless nickel immersion gold (ENIG) surface metallization. The joint morphology and the evolution of the joint microstructure were studied with X-ray inspection and scanning electron microscopy (SEM). We find heterogeneous responses were found across solders to TCT and aging tests. Partial cracking at the joint corner and inside IMC layers were observed in Sn5Sb after TCT, while SnAgCu5.5Sb, SnSbCuAg, and BiAgX® sustained less damage. However, the excessive IMC growth in the Sn-rich solder under 210 °C aging was the primary cause of joint degradation and cracking. During the aging test, electrolytic Ni metallization was mostly consumed and the material beneath the Cu layer was partially consumed. ENIG metallization samples resisted degradation for the same aging test. These results may indicate that lead-free solders are only suitable for power application under mild conditions.

Key words: Lead-free solder, Power Module, Thermal Cycling, Aging

INTRODUCTION

The usage of high power devices in electric vehicles and high temperature electronics requires reliable interconnections that can operate and sustain long term joint integrity at 175°C or higher. Current semiconductor materials such as Gallium Nitride and Silicon Carbide can already be used at operation temperatures of 175 °C and above. Additionally, Ag and Cu-sinter materials have high melting temperatures, excellent thermal and electrical conductivity, and high strength, even at operating temperatures of 200 °C [1]. The favorable properties of these sinter materials have prompted their use for power inverters/converters in die-attach applications. However, the use of Ag and Cu-sinter is limited in the rest of the power electronics industry due to their high material and processing costs.

Even traditional lead-free solders present challenges to these high power or high operating temperature devices. For traditional lead-free solders, the demanding operating conditions (175 °C or above) can lead to a homologous temperature as high as 0.91, increasing atomic diffusion and weakening creep resistance significantly [2]. Exposure to these conditions have adverse effects on the interconnective reliability of the solder as thermal migration under high temperatures promotes grain coarsening, excessive IMC growth, and phase segregation. Electro-migration may also occur if there is an electrical current applied to the solder interconnect. The current focus of this study is on the thermal fatigue performance and microstructural evolution of five lead-free solders: Sn3.5Ag, Sn5Sb, SnAgCu5.5Sb, SnSbCuAg, and BiAgX®. TCT and thermal aging were conducted to evaluate the performance of the selected solder materials.

EXPERIMENTAL

Sn3.5Ag, Sn5Sb, SnAgCu5.5Sb, SnSbCuAg, and BiAgX® were selected for this evaluation. All being lead-free solders, the samples all had liquidus temperatures ranging from 221

°C to 360 °C (shown in Table 1). The homologous temperatures at 175 °C for these alloys range from 0.71 to 0.91.

Table 1: Solidus and liquidus temperatures of the solders.

Alloy	Solidus (°C)	Liquidus (°C)
Sn3.5Ag	221	221
SnAgCu5.5Sb	224	233
Sn5Sb	235	240
BiAgX®	262	320
SnSbCuAg	>308	360

The testing vehicles were built in three different package configurations shown in Figure 1. The first consisted of 5x5 mm² Si die with a surface metallization of Ti/Ni/Ag onto a DBC substrate. The second and third used a 3x3mm² Cu plate as the die on top of a ceramic substrate. The Cu dies were placed in a 3x3 square pattern except for the bottom right corner exposing the solder material. The ceramic substrates had two different metallization's: Electrolytic-Ni-plated Cu and an ENIG surface finish layer over a Cu layer bonded directly to the ceramic.

The Si die on DBC testing vehicles were put into the TCT at -40 to 175 °C with a 10-minute dwell time resulting in a 52-minute cycle. These samples underwent 2000 cycles and were cross-sectioned for SEM imaging at both the 0th and 2000th cycle. The coefficient of thermal expansion (CTE) mismatch between the Si (3.0 ppm/°C) and Cu (16.7 ppm/°C) provided thermal stresses on the solder material for this study [3].

The Cu dies bonded to the ceramic substrates with the ENIG and electrolytic Ni metallization were run through thermal aging at 210 °C for 240 hours. Samples were cross-sectioned for SEM imaging at times 0, 72, and 240 hours.

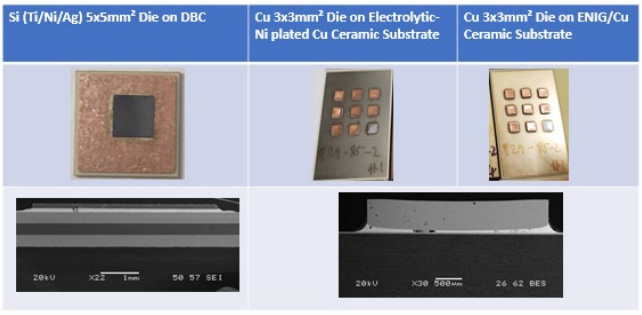

Figure 1: The Testing Vehicles fully assembled, 5x5mm² Si and 3x3mm² Cu dies bonded to their respective substrates, with images of the assembly and an overall SEM image of the joint.

RESULTS & DISCUSSION

Thermal Cycling Testing

Figure 2 shows the joint morphology of the Si/Cu-DBC of the samples after reflow. The 0-hour cross-sections show IMC formations along the interface and an absence of cracks on the edges of the joint.

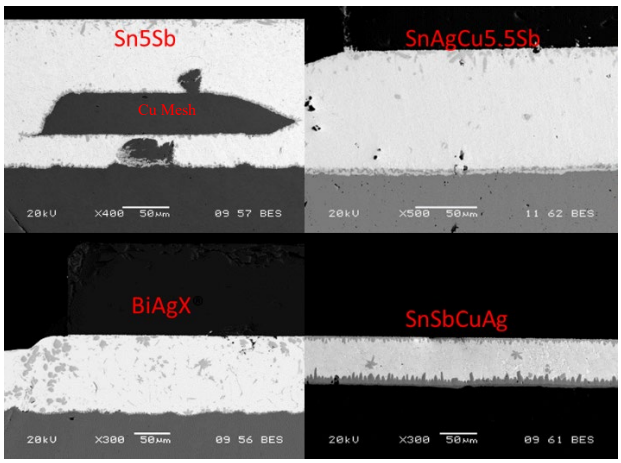

Figure 2: SEM Cross-section of the solder joints after reflow.

Two distinct IMCs formed at the Si die interface. The IMCs are Ni_3Sn_4 and $(CuNi)_6Sn_5$. Sn5Sb and BiAgX® possess the Ni_3Sn_4 interfacial reaction while, SnAgCu5.5Sb and SnSbCuAg contain the $(CuNi)_6Sn_5$. The solders that contain the $(CuNi)_6Sn_5$ IMC supplied the Cu from the bulk material. While the solders that possessed the Ni_3Sn_4 would have needed to diffuse Cu from the DBC to have it participate in a $(CuNi)_6Sn_5$ IMC on the Si die side.

The DBC supplied sufficient Cu to have a continuous Cu-based IMC at the interface such as Cu_6Sn_5 and Cu_3Sn. The IMC Cu_6Sn_5 was present in the solders Sn5Sb, SnAgCu5.5Sb and SnSbCuAg. The IMC Cu_3Sn was present in BiAgX® and SnSbCuAg. BiAgX® has a limited amount of Sn present within the solder material and the phase diagrams included in Figure 3 present that neither Bi or Ag form IMCs with Cu. Thus, forcing the dissolved Cu to react with the Sn in higher concentrations to form Cu_3Sn. SnSbCuAg has a relatively high concentration of Cu in the solder forming both Cu_6Sn_5 and Cu_3Sn which results in a subsequently larger IMC than the other solders investigated.

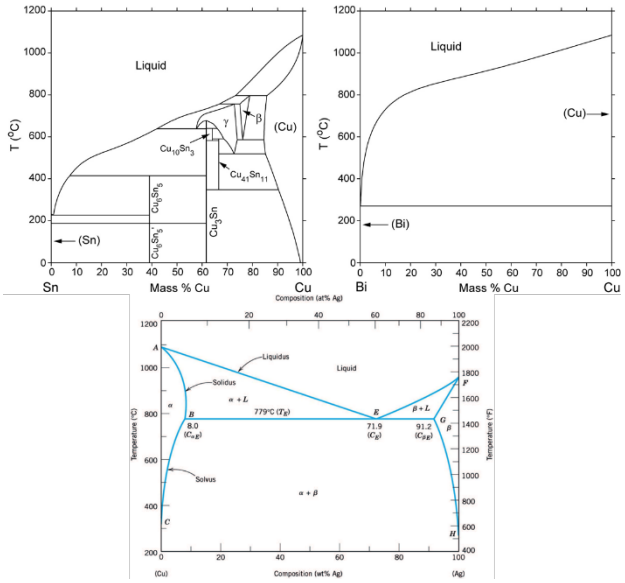

Figure 3: Phase Diagram of Sn-Cu, Ag-Cu, and Bi-Cu [4-6].

After the 2000 cycles in TCT all of the lead-free solders experienced limited crack propagation. Figure 4 compares the cracking of the solders where SnAgCu5.5Sb experienced the highest crack propagation from the corner followed by Sn5Sb, BiAgX®, and then SnSbCuAg. Fracture initiation observed in SnSbCuAg presented as vertical cracking away from the edge of the joint compared to the other three samples which exhibited cracking from the corner of the joint at the Si interface to towards the center of the joint.

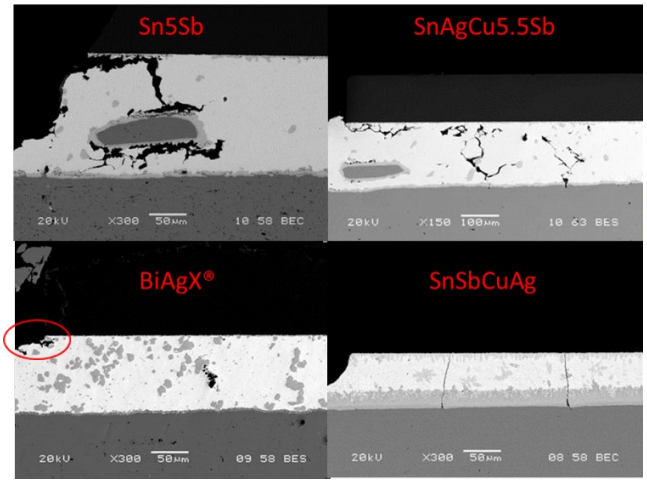

Figure 4: SEM imaging of the Crack propagation, the BiAgX® crack is indicated in red, within the lead-free solders after 2000 thermal cycles from -40 to 175 °C.

As a result of TCT, Sn5Sb experienced an IMC change on the Si die interface shown in Figure 5. The Ni_3Sn_4 IMC converted into $(CuNi)_6Sn_5$. The Cu required to change the interface IMC would have been supplied from the DBC and Cu mesh within the joint. Kirkendall voiding was observed within the new IMC that formed on the Si/Sn5Sb interface after TCT. Kirkendall voiding are dislocations within the solder joint due to unbalanced atomic diffusion between materials that appear as voiding [7]. As the dislocations grow in number and size, delamination and cracking may occur within the solder joint. The Sn5Sb/DBC interface experienced IMC growth and the formation of Cu_3Sn as well as increased cracking within the IMC shown in Figure 5. The solder SnAgCu5.5Sb experienced similar behavior to Sn5Sb with the exceptions that SnAgCu5.5Sb had $(CuNi)_6Sn_5$ and the coarsening of Ag_3Sn particles in the bulk solder that are not present in Sn5Sb.

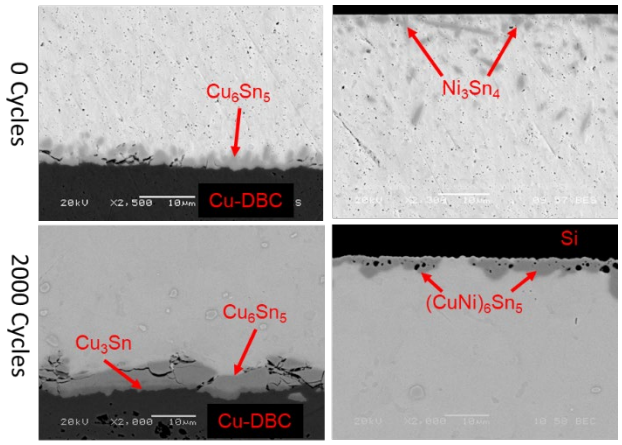

Figure 5: SEM imaging of the IMC interfaces for Sn5Sb at 0 cycles vs 2000 cycles for -40 to 175 °C TCT.

Figure 6 shows the solder morphology changes within SnSbCuAg. The Si die and the DBC interfaces experienced extensive IMC growth from SnSbCuAg as well as coarsening of the Ag_3Sn particles within the bulk solder.

The BiAgX® in Figure 7 showed little to no IMC growth on the Si or DBC interface after TCT at -40 to 175 °C for 2000 cycles. The Ag_3Sn IMCs within the bulk solder experienced coarsening (identified in Figure 7). On the Si interface the Ni_3Sn_4 IMC remained intact after cycling, and prevented a Ni-Bi intermetallic from forming with the Ni metallization layer.

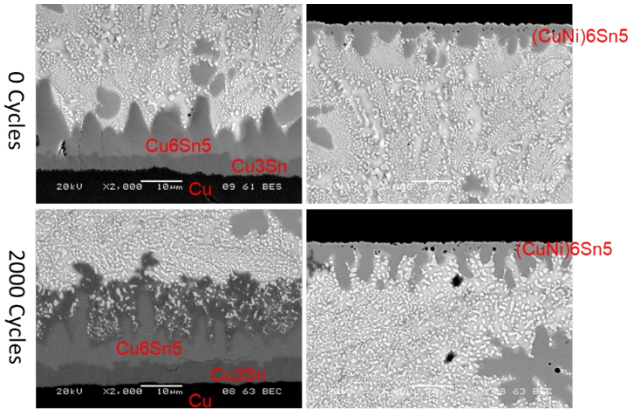

Figure 6: SEM imaging of the IMC interfaces for SnSbCuAg at 0 cycles vs 2000 cycles for -40 to 175 °C.

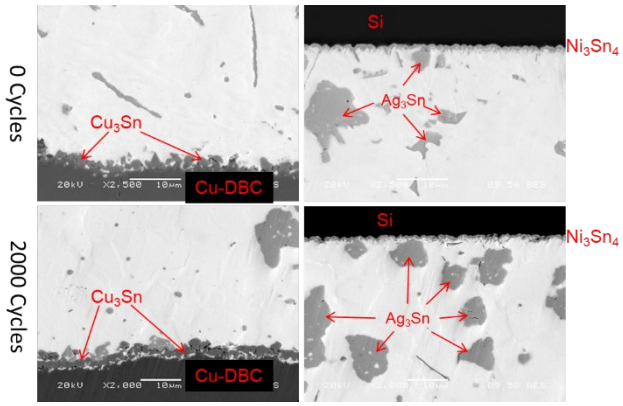

Figure 7: SEM imaging of the IMC interfaces for BiAgX® at 0 cycles vs 2000 cycles for -40 to 175 °C TCT.

Thermal Aging

Sn3.5Ag has the lowest melting point of the lead-free solders discussed. The homologous temperature for Sn3.5Ag at 210 °C is 0.98, indicating there is likely a large amount of atomic diffusion occurring within the solder joint. The microstructure evolution of Sn3.5Ag is shown in Figure 8, where the $(CuNi)_6Sn_5$ IMC grew rapidly at both the Cu die and electrolytic-Ni substrate even after 72 hours. The Cu die began to develop a Cu_3Sn IMC at the interface as well as coarsening of the Ag_3Sn particles in the solder joint. After 240 hours, the entire solder joint had been converted into IMCs with an Ag_3Sn phase separation. The Cu_3Sn at the Cu die interface continued to expand and the Ni metallization layer was critically consumed in some locations exposing the Cu layer. The ceramic substrates that contained the ENIG layer remained intact but Figure 9 shows the Sn matrix was still fully converted to IMC.

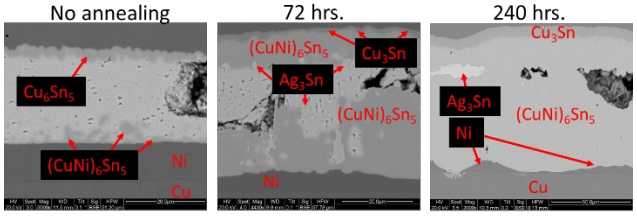

Figure 8: SEM imagining of microstructure evolution for Sn3.5Ag at 0, 72, and 240 hours for the Cu die on electrolytic-Ni-plated Cu substrate.

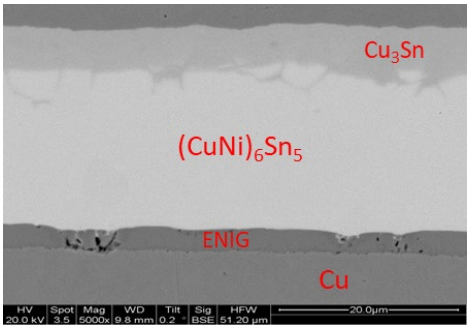

Figure 9: SEM imagining of microstructure evolution for Sn3.5Ag on the Cu die at 240 hours with the ENIG-plated Cu substrate.

After reflow Sn5Sb and SnAgCu5.5Sb showed similar IMC formation on the interfaces as seen in Figure 10. On the Cu die, both solders formed Cu_6Sn_5 while $(CuNi)_6Sn_5$ dominated the interface on the Ni substrate.

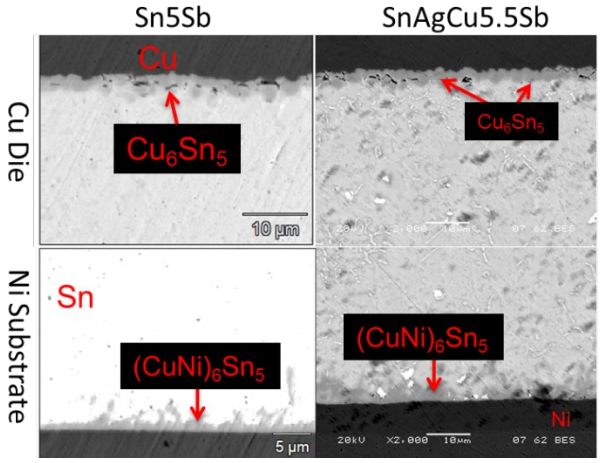

Figure 10: SEM of the joint morphology of Sn5Sb and SnAgCu5.5Sb after reflow for the Cu die electrolytic-Ni-plated Cu substrates.

After thermal aging at 210 °C for 240 hours, both Sn5Sb and SnAgCu5.5Sb showed cracking within the bulk solder that was not observed in the other lead-free solder alloys (Figure 11). The cracking within Sn5Sb and SnAgCu5.5Sb resulted from the severe IMC growth and Cu leaching from the Cu die after thermal aging. The crack propagation inside of the bulk solder for SnAgCu5.5Sb is more easily observed in Figure 12. The SnAgCu5.5Sb sample showed Ag_3Sn IMC coarsening and partial phase separation. The Sn matrix was consumed within the joint, degrading into $(CuNi)_6Sn_5$ IMC. Partial phase separation is defined as grain coarsening that has not formed a singular IMC phase such as the Ag_3Sn IMC in Figure 8 for Sn3.5Ag. The solder SnAgCu5.5Sb in Figure 12 shows an area of the joint that no longer contains Ag_3Sn >15 µm from the interface at the electrolytic Ni substrate and the Cu die.

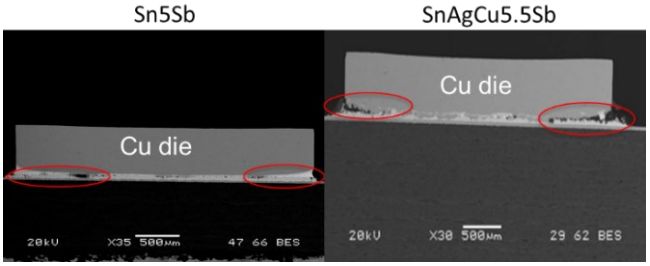

Figure 11: SEM of the joint for Sn5Sb and SnAgCu5.5Sb after thermal aging on the Cu die and electrolytic-Ni-plated Cu substrate testing vehicles. The red cracks are indicated in red.

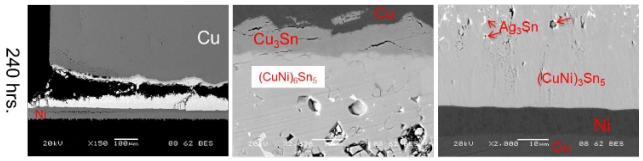

Figure 12: SEM of the SnAgCu5.5Sb corner, Cu die interface, and the Electrolytic- Ni substrate after 240 hours at 210 °C thermal aging.

The solder material, Sn5Sb, showed similar microstructure after aging to Sn3.5Ag and SnAgCu5.5Sb. In Figure 13, Sn5Sb formed a Cu_3Sn IMC at the Cu die interface where the Cu_6Sn_5 IMC was originally located at 0 hours aging. Phase separation is also visible in Figure 13. There is minimal Sn matrix left compared to the rest of the solder joint and the remaining Sn matrix is not continuous. The image with the scale bar of 50µm in Figure 13 shows crack propagation from within the remaining Sn matrix as well. The solder joint for Sn5Sb like SnAgCu5.5Sb and Sn3.5Ag has been fully converted into IMC. This conversion results in the solder joint overwhelmingly (>90%) consisting of $(CuNi)_6Sn_5$ and Cu_3Sn.

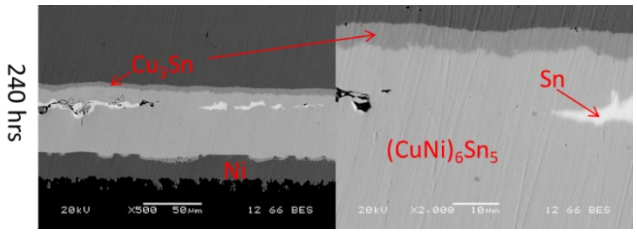

Figure 13: SEM of the Sn5Sb Cu die interface, and the electrolytic-Ni substrate after 240 hours at 210 °C thermal aging.

BiAgX®, designed with limited Sn in the solder, does not exhibit any of the excessive Cu_3Sn IMC growth during reflow or aging that occurred in the other lead-free solders. However, isolated Bi will not form any IMCs with Cu and Bi from BiAgX® will still grow the excessive IMCs with Ni as shown in the Figure 14 Bi-Ni phase diagram.

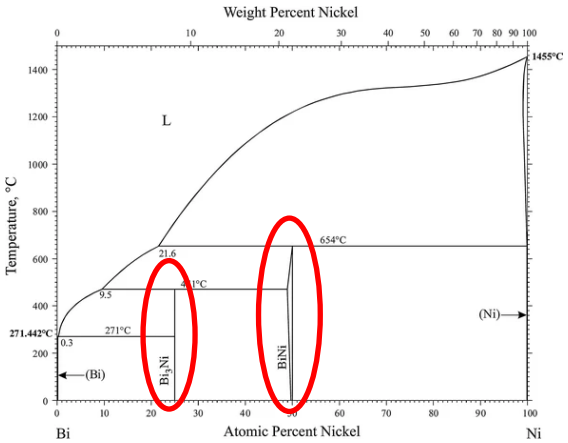

Figure 14: Phase Diagram of Bi-Ni, showing the IMCs of $NiBi_3$ and NiBi, that formed within the BiAgX® solder joint [8].

The cross-section of BiAgX® before cycling has the dispersed Ag_3Sn IMCs clearly shown in Figure 15. The interface on the Cu die side is Cu_3Sn. The electrolytic-Ni-plated Cu substrate for the aging samples formed some Ni_3Sn_4 IMCs at the interface also shown in Figure 12. After aging, the Ag_3Sn phase becomes much harder to find as well as any new IMC formations on the substrate. However, the Ni layer on the substrate was completely consumed when forming the NiBi IMCs after aging. Ni continued to leach into the solder joint also producing a large $NiBi_3$ IMC phase. Multiple layers of distinct phases can be distinguished in Figure 15, including BiNi, $NiBi_3$, BiNiO, a Bi-rich phase, and Cu_3Sn. For the ENIG-plated Cu substrates, the BiAgX® joint consumed the ENIG layer fully to form multiple IMC formations. The resulting layers consisted of BiN, Bi+NiBi3, and $(CuNi)_3Sn$ (Figure 16). The ENIG surface finish BiAgX® samples did not result in a BiNiO phase. For eutectic Sn-Bi solders, there is enough Sn within the solder joint to prevent Bi-Ni IMCs from forming even at prolonged high temperatures [9].

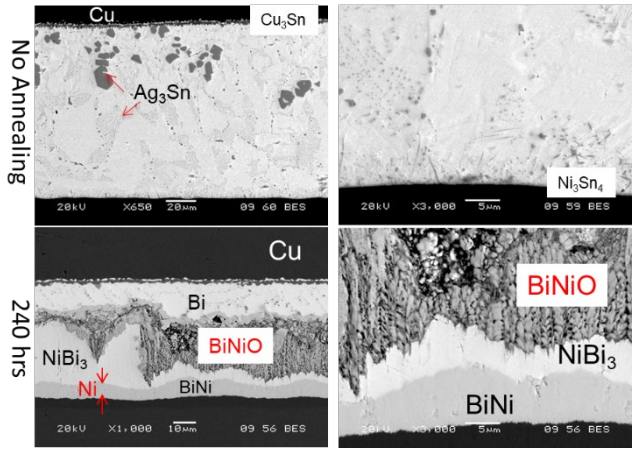

Figure 15: SEM of BiAgX® joint morphology showing the bonding of the Cu die to the electrolytic Ni-plated Cu substrate before and after 240 hours. Thermal aging at 210 °C pointing out IMCs within the solder.

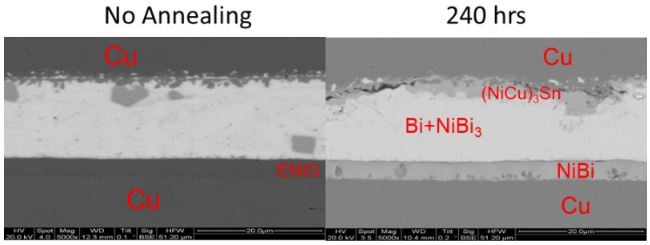

Figure 16: SEM of BiAgX® joint morphology showing the bonding of the Cu die to the ENIG-plated Cu substrate, before and after 240 hours Thermal aging at 210 °C pointing out IMCs within the solder.

CONCLUSION

Traditional lead-free solders are not suitable for applications involving operating temperatures of 175 °C or higher. Due to excessive IMC growth, grain coarsening, and phase segregation, the tested lead-free solders are not suitable for

these high temperature or power applications. After 240 hours at 210 °C, all the solders experienced joint-encompassing IMC growth, grain coarsening, phase separation, and two of the solders experienced continued crack propagation. TCT after 2000 cycles at -40 to 175 °C for Sn5Sb, SnAgCu5.5Sb, BiAgX®, and SnSbCuAg resulted in notable IMC growth for all samples and corner cracking within the bulk solder for all except SnSbCuAg. SnSbCuAg did, however, experience vertical cracking toward the center of the joint at 2000 cycles. Additionally, the TCT resulted in micro-crack propagation within the IMC attaching to the DBC for Sn5Sb, SnAgCu5.5Sb, and BiAgX®. These results indicate that current lead-free solders are only suitable for power applications under mild testing and operating conditions.

REFERNCE

1. M. Nowottnick, A. Novikov, T. Herberholz, and D. Feil "JOINING TECHNOLOGIES FOR HIGH TEMPERATURE ELECTRONICS", *Harsh Environments Conference 2018 Proceedings*, 2018.
2. G.E. Dieter, Mechanical Metallurgy, 3rd Edition, McGraw-Hill, Inc., 1986.
3. F. Cverna, "ASM Ready Reference: Thermal properties of metals", *ASM International,* P.10-23, 2002.
4. A. Kawecki, T. A. Knych, E. Sieja-Smaga, A. Mamala, ect. "Fabrication, properties and microstructures of high strength and high conductivity copper-silver wires" *Archives of Metallurgy and Materials Volume 57 Issue 4*, P.1261-1270, 2013.
5. O. Teppo, J. Niemelä and P. Taskinen, "Bi-Cu System" Thermochim. Acta 173 (1990) 137-150: Full thermodynamic assessment.
6. J.-H. Shim, C.-S. Oh, B.-J. Lee and D.N. Lee, Z. "Thermodynamic description of the Cu-Sn system" Metallkde. 87 (1996) 205-212: Full thermodynamic assessment.
7. F. Batieha, F. Feyissa, S. Hamasha, S. Shirazi, L. Wentlent, P. Oguto, N. Dimitrov, E. Fay, and P. Borgesen, "'Kirkendall' Voiding in 2.5/3D Assembly Microjoints," Medical Electronics Symposium Conference Proceedings, SMTA (Edina, MN: Surface Mount Technology Association), 2014
8. P. Nash, "The Bi-Ni (Bismuth-Nickel) System", *Bulletin of the Alloy Phase Diagrams 6,* P.345-347, 1985.
9. Tao, W. & Chen, Chong & Ho, Cheng-En & Chen, W. & Kao, C.., "Selective Interfacial Reaction between Ni and Eutectic BiSn Lead-Free Solder". *Chemistry of Materials*. P.1051-1056, 2001.